J Mater Sci: Mater Med (2007) 18:1895–1905
DOI 10.1007/s10856-007-3092-8

Proliferation of osteoblasts and fibroblasts on model surfaces of varying roughness and surface chemistry

Helmut Schweikl · Rainer Müller · Carsten Englert · Karl-Anton Hiller · Richard Kujat · Michael Nerlich · Gottfried Schmalz

Published online: 2 June 2007

Abstract Physical and chemical properties of the surfaces of implants are of considerable interest for dental and orthopedic applications. We used self-assembled monolayers (SAMs) terminated by various functional chemical groups to study the effect of surface chemistry on cell behavior. Cell morphology and proliferation on silicon wafers of various roughnesses and topographies created by chemical etching in caustic solution and by corundum sandblasting were analyzed as well. Water contact angle data indicated that oxidized wafer surfaces displayed high hydrophilicity, modification with poly(ethylene glycol) (PEG) created a hydrophilic surface, and an amino group (NH_2) led to a moderately wettable surface. A hydrophobic surface was formed by hydrocarbon chains terminated by CH_3, but this hydrophobicity was even further increased by a fluorocarbon (CF_3) group. Cell proliferation on these surfaces was different depending primarily on the chemistry of the terminating groups rather than on wettability. Cell proliferation on CH_3 was as high as on NH_2 and hydrophilic oxidized surfaces, but significantly lower on CF_3. Precoating of silicon wafers with cell culture serum had no significant influence on cell proliferation. Scanning electron microscopy indicated a very weak initial cell-surface contact on CF_3. The cell number of osteoblasts was significantly lower on sandblasted surfaces compared with other rough surfaces but no differences were detected with 3T3 mouse fibroblasts. The different surface roughnesses and topographies were recognized by MG-63 osteoblasts. The cells spread well on smooth surfaces but appeared smaller on a rough and unique pyramid-shaped surface and on a rough sandblasted surface.

H. Schweikl (✉) · K.-A. Hiller · G. Schmalz
Department of Operative Dentistry and Periodontology, Dental School, University of Regensburg, Regensburg 93053, Germany
e-mail: helmut.schweikl@klinik.uni-regensburg.de

R. Müller
Institute of Physical and Theoretical Chemistry, University of Regensburg, Universitätsstrasse 31, Regensburg 93053, Germany

C. Englert · R. Kujat · M. Nerlich
Department of Trauma Surgery, Medical School, University of Regensburg, Regensburg 93053, Germany

Introduction

The formation and properties of an implant-tissue interface depend on the physico–chemical properties and the cell biocompatibility of an implant material. Biocompatibility involves two different aspects, biological safety and biofunctionality. The analysis of biological safety includes testing of the cytotoxic, mutagenic or carcinogenic and immuno-allergological potential. The surface of a biomaterial, on the other hand, is the major parameter influencing its biofunctionality. Initial cell attachment to a material surface determines the subsequent processes like cell adhesion, spreading, morphology, migration, proliferation and differentiation [1, 2]. Biomaterial surfaces formed by different biomedical polymers, metals or alloys, and ceramics possess a high degree of surface heterogeneity including type and density of functional chemical groups, hydrophilic and hydrophobic areas, surface texture and roughness. To study the effect of surface chemistry on adhesion and proliferation of tissue cells, self-assembled monolayers (SAMs) of various alkanethiols and alkylsilanes were used as model surfaces independent of the particular biomaterial. For instance, hydrophilic and

hydrophobic properties were created and controlled on these model surfaces by termination with groups like COOH and NH_2 or CH_3, CF_3, PEG (poly(ethylene glycol)) and OH. It appears as if hydrophilic surfaces supported adhesion of various cell types whereas hydrophobic surfaces often inhibited the interaction between cells and artificial surfaces [3–9]. Surface topography is another major factor, which determines the functional activity of cells in contact with a biomaterial. There is growing evidence that micrometer and nanometer scale topographies may be able to modify different aspects of cell behavior like cell adhesion, morphology, proliferation, and differentiation, as well as the production of local factors and microenvironments [10–15]. The variation in results obtained thus far may depend on the roughness amplitude and the method used to produce the surface topography and texture [14–18].

Physico–chemical modification of the surface of implant materials are of considerable interest for the restoration of human tissues including cartilage and bone in dental and orthopedic applications. Here, we analyzed cell activities on smooth SAMs of alkylsilanes terminated by functional end groups including NH_2, CH_3, CF_3, and PEG in addition to oxidized surfaces. Also, varying roughness of wafer surfaces with unique textures were created by chemical etching in caustic solution for various time periods. Our analyses focused on the characterization of the influence of hydrophilic, hydrophobic, smooth, and rough surfaces on cell proliferation, morphology, and the formation of contacts at the material-cell interface. The morphological properties were analyzed using an environmental scanning electron microscope (ESEM). Since cellular adhesion was mediated by a protein layer adsorbed from fluids like blood and interstitial fluid, the smooth and rough silicon wafer surfaces were precoated with serum proteins. We chose osteoblasts and fibroblasts as cell lines due to their relevance to implants in cartilage and bone tissues.

Materials and methods

Chemicals

N-(triethoxysilylpropyl)-*O*-poly(ethylene glycol)urethane (PEG), *n*-octyltriethoxysilane (OTS), 3-aminopropyltriethoxysilane (APS) and (heptadecafluoro-1,1,2,2-tetrahydrodecyl)trichlorosilane (HFS) were obtained from ABCR (Karlsruhe, Germany). Acetone, ethanol, nitric acid, and toluene were purchased from VWR International (Darmstadt, Germany) and Riedel-de-Haën (Seelze, Germany). Minimum essential medium Eagle (MEME) was purchased from ATCC (no. 30-2003). Fetal bovine serum (FBS) was obtained from PAN-Biotech (Aidenbach, Germany). Penicillin/streptomycin and trypsin came from Life Technologies, Gibco BRL (Eggenstein, Germany). Crystal violet was purchased from Sigma-Aldrich (Taufkirchen, Germany). Water was purified by ultrafiltration using an apparatus from Millipore Corp. (Billerica, MA, USA).

Preparation of model surfaces on silicon wafers

Single-side polished silicon wafers (*n*-type; phosphor-doped; 1–10 Ωcm resistivity; 575–675 μm thickness) were purchased from Wafer World Inc. (West Palm Beach, FL, USA). The wafers were cut into 10 × 10 mm squares using a special wafer saw. Wafer surfaces were cleansed by successive sonicating of the specimens in acetone, toluene, ethanol, and water for 5 min.

To create hydroxyl groups providing hydrophilic surfaces, wafers were sonicated in 32.5% nitric acid solution for 30 min at room temperature. Excess acid was removed by repeated water rinsing, and the oxidized wafers were stored in 0.1% sodium azide solution. Further chemical modification of the wafer surfaces was achieved by coating with SAMs which were terminated by the following chemical functions: PEG, NH_2, CH_3, or CF_3. Dried wafers were silanized by boiling in toluene solutions containing 15 mg/ml of either *N*-(triethoxysilylpropyl)-*O*-poly(ethylene glycol)urethane (PEG), APS, OTS, or HFS for 3 h. Next, the wafers were sonicated consecutively in pure toluene, chloroform, and methanol, then dried in a nitrogen stream, and finally stored in a vacuum desiccator.

The physical structure of the silicon wafer surface was modified as follows. One group of specimens was roughened by abrasive blasting using corundum particles with an average size of 50 μm (Harnisch & Rieth, Germany). The abrasive was applied with a working pressure of 2 bar by a PG 360/3 sand-blasting machine (Harnisch & Rieth, Germany). Here, the nozzle was moved by hand at a constant distance of about 3 cm under an angle of about 30° to the wafer surface for 30 s per wafer. A second and a third group of specimens were subjected to caustic etching processes in 10% aqueous potassium hydroxide solution [19]. Wafers were incubated in the alkaline solution at 80 °C for either 5 or 60 min, thus resulting in different etching rates. The specimens were then rinsed with water to remove excessive alkali. Hydrophilic surfaces were created by oxidation in nitric acid as described above.

Characterization of the wafer surfaces

Advancing water contact angles (θ_a) on the modified wafer surfaces were measured using the sessile drop method on a P1 goniometer from Erna Inc. (Japan). 2 μL-droplets were

advanced toward the samples by a syringe tip until the droplets made contact with the sample surfaces. Contact angles were read on one side of 10 droplets which were deposited on five different wafers for each surface modification (Table 1). X-ray photoelectron spectra (XPS) were recorded using a PHI 5700 from Physical Electronics Co. (USA) by application of monochromatic Al-Kα radiation under an analytical angle of 45°. Surface element composition was calculated by considering all identified signals of the survey after linear deduction of the background (Table 1). The roughness of the physically and chemically altered structures of the silicon wafer surfaces was analyzed using a perthometer S6P from Mahr GmbH (Germany). Twelve wafers were characterized for each modification and results are expressed as the arithmetic average peak-to-valley value (R_a) (Table 1).

Scanning electron microscopy (SEM)

The surface of the wafer specimens was analyzed using a FEI Quanta 400F (Eindhoven, Netherlands) environmental scanning electron microscope (ESEM). Wafer specimens were placed directly into the SEM chamber for surface structure analyses. The spreading of MG-63 osteoblasts on humid silicon wafer surfaces was investigated by SEM using the low vacuum mode at a pressure of 1.5 Torr at room temperature. The specimens on the stage were tilted by 30°. A 30-µm incident beam aperture was typically used with a spot size of 4 nm, an accelerating voltage of 4 kV, and a large field detector (LFD) was used to image the cells.

Cell culture experiments

Cell culture and cell proliferation on silicon wafers

Human MG-63 osteoblasts (ATCC CRL-1427) and mouse 3T3 fibroblasts (ATCC CRL 1658) were maintained in minimal essential medium Eagle (MEME) supplemented with 10% FBS, and penicillin-streptomycin at 37 °C in a humidified 5% CO_2/95% air atmosphere. The cells were detached by trypsinization, collected by centrifugation, and resuspended in culture medium. Sterilized wafer specimens (10 × 10 mm) were individually placed into single wells of a 24-well plate (Sarstedt, Germany). Half of the specimens were precoated by incubation in 0.5 ml fetal bovine serum for 60 min at 37 °C. Subsequently, the wafer specimens were washed three times with phosphate-buffered saline (PBS). After that, MG-63 osteoblasts and 3T3 fibroblasts (1×10^4 cells/well) were seeded in complete cell culture medium onto coated and uncoated wafer specimens. Tissue culture polystyrene (PS) (Sarstedt, Germany) served as a reference material. The cells were then incubated for 2, 5, and 8 days at 37 °C in a humidified 5% CO_2/95% air atmosphere. After these various incubation periods, the cell culture medium was removed, the cells were washed twice in PBS, and fixed in 1% glutaraldehyde. These wafer specimens were then transferred to a new 24-well plate, and the number of cells on each surface was determined using a crystal violet assay (see below) [20]. To calculate the cell numbers on the wafer specimens and on tissue culture polystyrene, standard curves were established by plating eight cell numbers between 2.5 and 150×10^3 cells per well and performing the crystal violet assay. Each standard cell number was used in quadruplicate, and individual standard curves were created in each single experiment.

The morphology of MG-63 osteoblasts on various surfaces of silicon wafers was also characterized by SEM. The cells (6×10^4/well) were first seeded onto the wafer specimens (10 × 10 mm) which were then placed in wells of a 24-well plate. After incubation periods of 5 h, or 2, 5, and 8 days, the cells were washed twice in PBS, fixed in 1% glutaraldehyde for 30 min at room temperature, and then stored in PBS at cold temperatures.

Table 1 Surface roughness as described by the arithmetic average peak-to-valley values (R_a), surface element composition as obtained by XPS measurements and advancing water contact angle of silicon wafers after surface modification

Modification	R_a [µm]	XPS [At-%]					θ_a [°]
		O	C	N	F	Al	
Polished, HNO_3 oxid.	0.04 (0.04–0.04)	32.4	20.4	0.8	–	–	11 (10–15)
Sandblasted, HNO_3 oxid.	1.72 (1.38–1.95)	42.6	12.6	0.9	–	5.0	<10
KOH 5 min, HNO_3 oxid.	0.17 (0.11–0.23)	33.4	24.0	1.1	–	–	17 (16–17)
KOH 60 min, HNO_3 oxid.	1.58 (1.41–1.73)	32.4	27.3	1.4	–	–	<10
Polished, PEG modified	0.04 (0.04–0.04)	39.6	21.4	1.5	–	–	39 (37–42)
Polished, APS modified	0.04 (0.04–0.04)	31.8	33.4	4.7	–	–	54 (52–56)
Polished, OTS modified	0.04 (0.04–0.04)	39.3	17.3	0.5	–	–	76 (66–89)
Polished, HFS modified	0.04 (0.04–0.04)	17.4	17.5	0.4	50.4	–	112 (108–116)

Values for R_a and θ_a are shown as medians (25–75% quartiles)

Crystal violet assay

The cells fixed on the wafer specimens were stained with 300 μL crystal violet solution (0.02% in water) for 15 min at room temperature. Next, the crystal violet solution was removed, and each well was washed thoroughly with tap water. The wafer specimens were transferred to a new well, and the amount of crystal violet bound to the cells on the wafer specimens was dissolved with 360 μL 70% ethanol for 3 h under gentle shaking. An aliquot (150 μL) of this solution was then transferred to a single well of a 96-well plate, and optical densities were measured at 590 nm in a multiwell spectrophotometer (EL311, Biotek Instruments GmbH, Bad Friedrichshall, Germany). In addition, the original crystal violet solution was diluted 1:2 and 1:3, and analyzed photometrically to rule out a detection limit of cell numbers due to the saturation of staining. The optical density readings of cell numbers used to create a standard curve were subjected to linear regression analyses using Sigma Plot (Systat Software, Point Richmond, CA, USA).

Statistical analysis

The cell numbers on the various silicon wafers were analyzed in quadruplicate (4 specimens) in each experiment, and each experiment was repeated at least once. The absolute cell number on each wafer specimen was calculated from a standard curve as described. Differences between median values of cell numbers on the various wafer surfaces were statistically analyzed using the Mann–Whitney-U-test (SPSS/PC+, Vers. 13.0 SPSS, Chicago, IL, USA) for pair-wise comparisons among groups at the 0.05 level of significance.

Results

Surface modification of silicon wafers

Chemical etching in caustic solution and corundum sandblasting created silicon wafer surfaces of varying surface topography and roughness. Significant differences in the surface structure and the arithmetic average peak-to-valley values (R_a) have been found depending on the applied roughening technique. While sandblasting resulted in a rock-like surface structure with sharp ridges and edges, etching in KOH solution created somewhat regularly shaped pyramids (Fig. 1). The size of the pyramids and, therefore, the value for the surface roughness increased with respect to the length of caustic etching time. Although sandblasting and KOH etching for 60 min resulted in completely different surface topographies, statistically significant differences were not found between the average surface roughness of both surfaces ($p = 0.63$). In contrast, the R_a values for all other surfaces were significantly different ($p = 0$). XPS measurements revealed that abrasion with corundum particles led to an incorporation of aluminum into the outer surface layers of the silicon wafer. No remnants of the KOH etching procedure could be found, while nitric acid oxidation caused incorporation of some nitrogen into the wafer surfaces. Roughened and oxidized wafer surfaces displayed high hydrophilicity with advancing water contact angles below 20° (Table 1).

Immobilization of silane molecules to the oxidized surfaces led to an increase in the advancing water contact angle (θ_a). The introduction of PEG-containing silane molecules increased θ_a only slightly and the surfaces retained a hydrophilic character. After immobilization of the amino group containing silane (APS) a positively charged surface with a medium water contact angle was obtained. Surfaces with hydrophobic properties were obtained after immobilization of hydrocarbon chains (OTS) to the wafers. This hydrophobicity was even further increased by the introduction of fluoroalkyl chains (HFS) onto the wafers. The values for the water contact angle were significantly different ($p = 0.000$) between all of the five different surface modifications. Immobilization of silane molecules did not alter the roughness of the wafer surfaces. The successful attachment of the different silane molecules could additionally be monitored by the increase in the surface content or the introduction of relevant elements as demonstrated by XPS measurements (Table 1).

Cell proliferation on self-assembled monolayers (SAMs)

Cell proliferation of human MG-63 osteoblasts and mouse 3T3 fibroblasts on silicon wafers covered with SAMs was determined. The measurement of cell numbers 2, 5, and 8 days after cell seeding in complete culture medium indicated the ability of the cells to attach, proliferate, and survive on the various wafer surfaces.

In the absence of serum precoating of the wafer surfaces, the number of MG-63 osteoblasts on the various SAMs was not significantly different after 2 days (Fig. 2A). However, significantly more cells adhered to polystyrene tissue culture plates (PS). Proliferation of MG-63 cells was observed on all wafer surfaces after a time period of 2–8 days. Five days after seeding, the highest cell numbers on SAMs were detected on oxidized surfaces (Ox) and NH_2-surfaces (APS), while only about half this number was present on CH_3 (OTS) and PEG-modified wafers. Even lower cell proliferation was identified on the highly hydrophobic fluorocarbon surfaces (CF_3 = HFS) (Fig. 2A). The number of cells on oxidized surfaces increased by about threefold between days 5 and 8 after seeding, and the

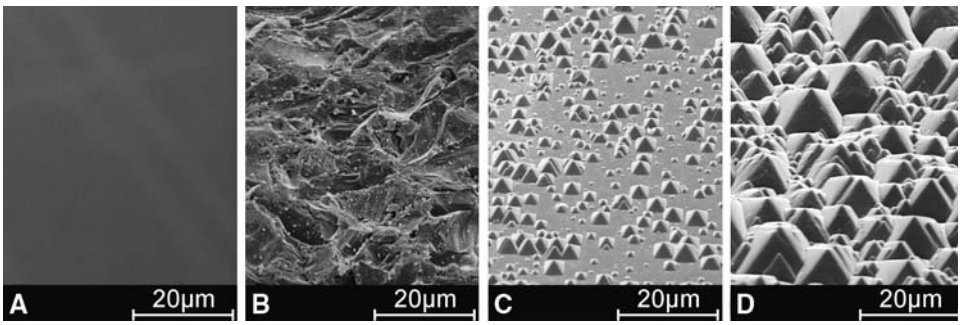

Fig. 1 Scanning electron micrographs of wafer surfaces after application of physically and chemically-based roughening procedures: Untreated polished wafer (**A**), wafer after sandblasting with 50 µm corundum particles (**B**), wafer after 5 min KOH etching (**C**), wafer after 60 min KOH etching (**D**). All surfaces were oxidized by incubation in nitric acid solution

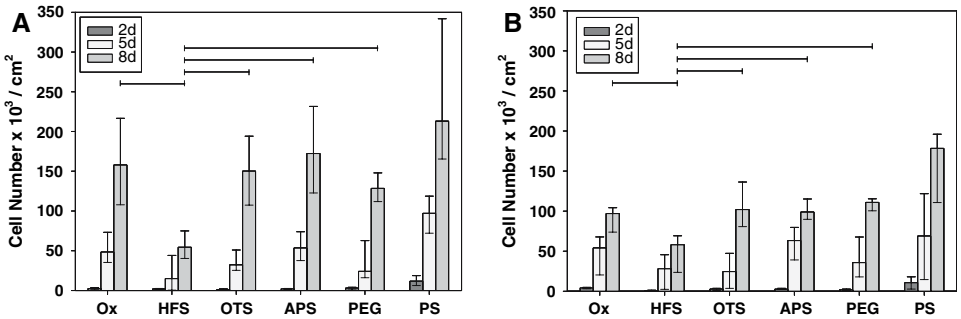

Fig. 2 Proliferation of MG-63 osteoblasts on SAMs. Absolute cell numbers were determined on pure SAMs (**A**) and on wafer surfaces precoated with serum (**B**). Ox = oxidized wafer surface, HFS = heptadecafluoro-1,1,2,2-tetrahydrodecyl)trichlorosilane, OTS = *n*-octyltriethoxysilane, APS = 3-aminopropyltriethoxysilane, PEG = *N*-(triethoxysilylpropyl)-*O*-poly(ethylene glycol)-urethane, PS = tissue culture polystyrene. The columns represent medians (25% and 75% percentiles) (n = 5–8), and the horizontal lines indicate statistically significant differences between cell numbers on the indicated surfaces

same level of cell proliferation was observed on APS and OTS. A lower number of cells were present on the PEG surface, but this difference was not significant. Cell proliferation on HFS was very slow and significantly lower compared with all other surfaces after an incubation period of 8 days (Fig. 2A). The cell numbers on the serum-precoated, oxidized OTS and APS surfaces were significantly lower compared with non-coated specimens. Again, cell proliferation on serum-coated HFS surfaces was still significantly lower compared with all other surfaces at day 8 after seeding (Fig. 2B).

The morphology of MG-63 osteoblasts on oxidized hydrophilic surfaces and hydrophobic HFS-coated surfaces was also analyzed by SEM (Fig. 3). There was a clear evolution of the cell morphology on these surfaces between 5 h and 8 days after seeding. The few osteoblasts seen immediately after seeding appeared rounded, not completely spread, but with contact to the oxidized surface through filopods (Fig. 3A). At day 2 after seeding the osteoblasts appeared extremely flattened, with clearly visible filopods and some cell contacts (Fig. 3B). Finally, a tightly packed layer of osteoblasts was reached at day 8 after seeding (Fig. 3C and D). In contrast, MG-63 osteoblasts appeared in very low numbers on HFS after 5 h, and the cells were small, not well spread but extremely rounded with almost no visible contact to the surface (Fig. 3E). After 2 days, the number of cells had increased, although not all cells appeared well spread, some cells showed a spindle-like morphology, and only few filopods were visible (Fig. 3E and D). However, the cell density also increased with time on HFS, and a confluent cell monolayer was present 8 days after seeding (Fig. 3G and H).

The 3T3 fibroblasts also proliferated on wafer surfaces, and the distribution of the number of fibroblasts on the various SAMs was very similar to that observed with MG-63 osteoblasts. However, the proliferation rate of 3T3 fibroblasts was apparently higher compared to MG-63 osteoblasts since the largest increase in cell number on all surfaces was observed between day 2 and day 5 after seeding (Fig. 4A). Compared with these increases, only a slightly higher cell number was observed between days 5 and 8 indicating cell layers near confluence. Cell proliferation of the fibroblasts was significantly higher on APS but significantly lower on HFS compared with all other surfaces (Fig. 4A). Precoating of the silicon wafer surfaces with cell culture serum had no detectable effect on the

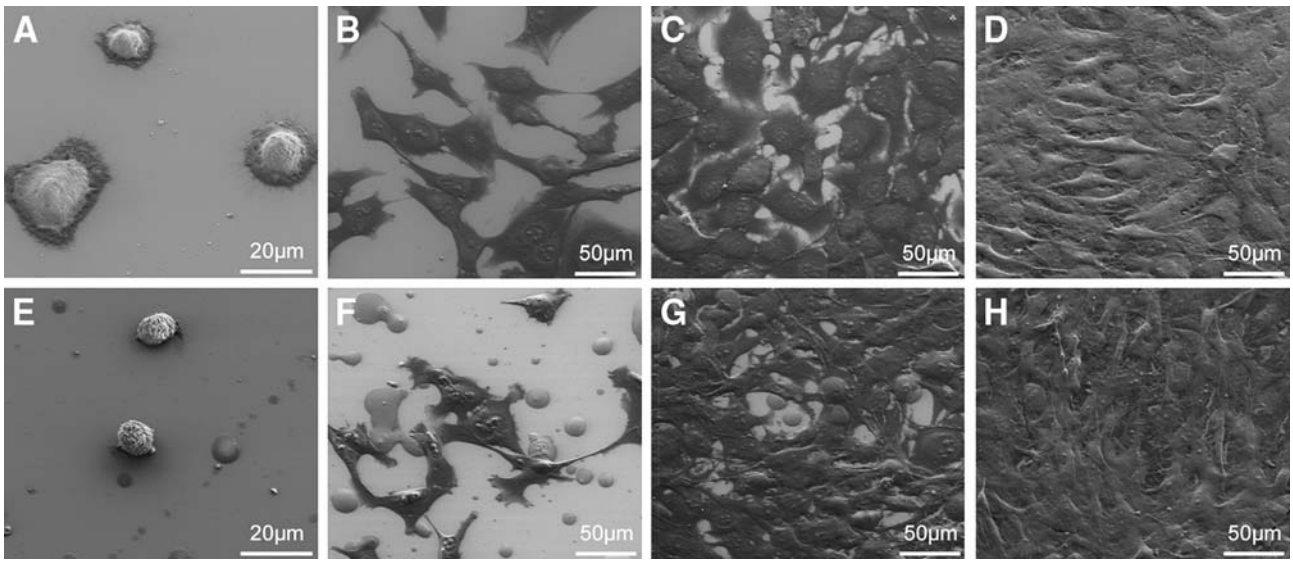

Fig. 3 Scanning electron micrographs of human MG-63 osteoblasts on silicon wafers. The cell morphology was analyzed between 5 h and 8 days after seeding onto oxidized (**A**–**D**) and HFS-coated (**E**–**H**) surfaces. Rounded cells with contact to the oxidized surface are visible immediately (5 h) after plating (**A**). The cells appear extremely flattened with filopods indicating close contact to the material surface, and the cell density increased between days 2 (**B**) and 5 (**C**). A confluent cell layer was formed at day 8 after seeding (**D**). Only a few small, and extremely rounded osteoblasts appeared on the HFS surface after 5 h (**E**). The cell contact to the surface was enhanced after 2 days (**F**), but there were morphological differences between cells grown on oxidized and HFS surfaces. The cell density also increased on HFS after 5 days (**G**), and a confluent cell monolayer was formed after 8 days (**H**)

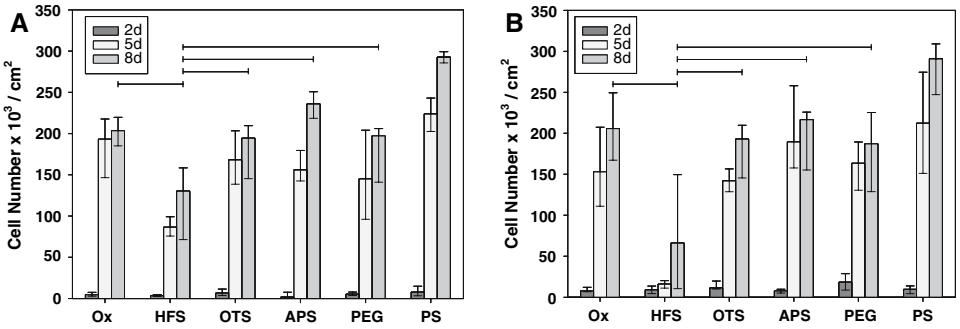

Fig. 4 Proliferation of 3T3 mouse fibroblasts on SAMs. Absolute cell numbers were determined on pure SAMs (**A**) and on wafer surfaces precoated with serum (**B**). Ox = oxidized wafer surface, HFS = heptadecafluoro-1,1,2,2-tetrahydrodecyl)trichlorosilane, OTS = *n*-octyltriethoxysilane, APS = 3-aminopropyltriethoxysilane, PEG = *N*-(triethoxysilylpropyl)-*O*-poly(ethylene glycol)-urethane, PS = tissue culture polystyrene. The columns represent medians (25% and 75% percentiles) (n = 6–8), and the horizontal lines indicate statistically significant differences between cell numbers on the indicated surfaces

proliferation of the fibroblasts except for the HFS surface. 3T3 cell proliferation was inhibited on this hydrophobic surface until day 5 after cell seeding (Fig. 4B).

Cell proliferation on rough silicon wafers

In the absence of serum precoating, the number of osteoblasts attached to smooth oxidized surfaces (Ox), sandblasted (SB), and rough surfaces created by etching silicon wafers in a KOH solution for 5 (KOH 5) and 60 min (KOH 60) was not significantly different after 2 days (Fig. 5A). All surfaces supported the proliferation of MG-63 cells during the observation period of 8 days, but proliferation rates varied depending on the wafer surface. Although no significant differences were found between cell numbers on smooth oxidized surfaces (Ox) and those surfaces etched with KOH, the number on sandblasted surfaces (SB) was significantly lower at day 8 after seeding (Fig. 5A). Precoating the rough surfaces with cell culture serum increased MG-63 cell proliferation on SB surfaces. Notably, cell proliferation was significantly higher on polystyrene tissue culture plates (PS) compared with all other surfaces (Fig. 5A and B). Proliferation of the 3T3 fibroblasts was very similar on all wafer surfaces independent of the presence of precoating with serum. No significant reduction in cell proliferation on sandblasted surfaces was detected. The number of 3T3 cells on PS was significantly higher than on the rough wafer surfaces (Fig. 6A and B).

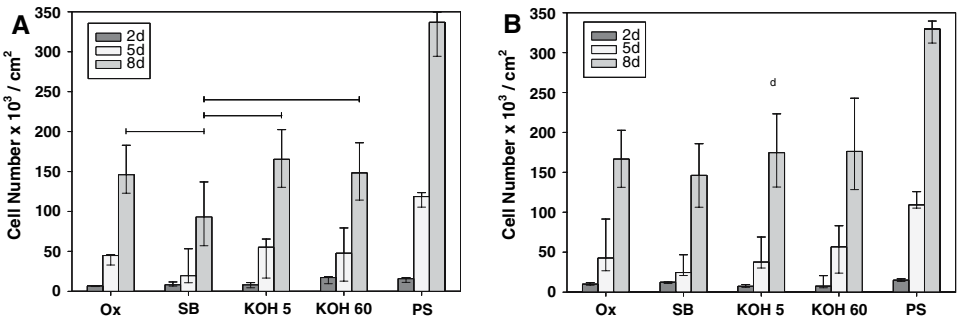

Fig. 5 Proliferation of MG-63 osteoblasts on rough silicon wafer surfaces. Absolute cell numbers were determined on pure wafer surfaces (**A**) and on surfaces precoated with serum (**B**). Ox = oxidized smooth wafer surface, SB = sandblasting, KOH 5 = caustic etching processes in 10% aqueous potassium hydroxide solution for 5 min, KOH 60 = caustic etching processes in 10% aqueous potassium hydroxide solution for 60 min. PS = tissue culture polystyrene. The columns represent medians (25% and 75% percentiles) (n = 5–8), and the horizontal lines indicate statistically significant differences between cell numbers on the indicated surfaces

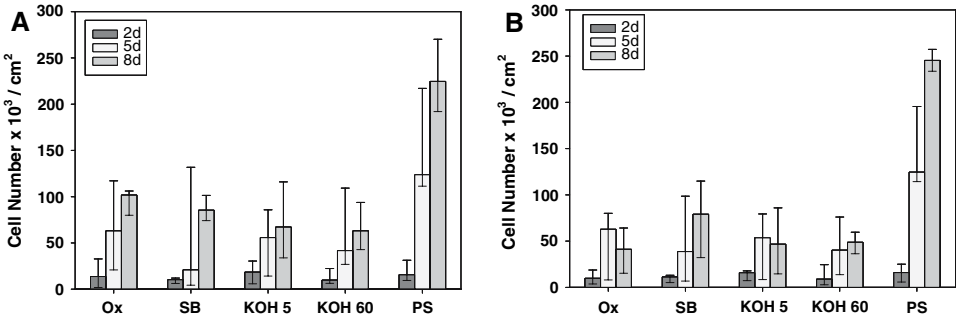

Fig. 6 Proliferation of 3T3 mouse fibroblasts on rough silicon wafer surfaces. Absolute cell numbers were determined on pure wafer surfaces (**A**) and on surfaces precoated with serum (**B**). Ox = oxidized smooth wafer surface, SB = sand blasting, KOH 5 = caustic etching processes in 10% aqueous potassium hydroxide solution for 5 min, KOH 60 = caustic etching processes in 10% aqueous potassium hydroxide solution for 60 min, PS = tissue culture polystyrene. The columns represent medians (25% and 75% percentiles) (n = 5–8)

Representative SEM images showed morphological differences between MG-63 cells grown on smooth and micro-structured surfaces. On the smooth surface, the cells appeared well spread and very flat indicating close contact to the wafer surface. The cells were attached by numerous filopods to the even surface, and they formed early cell-cell contacts (Fig. 7A). Etching in KOH solution for a short period of time created surfaces with a few small, regularly shaped pyramids which were well separated on an otherwise smooth wafer surface. The MG-63 osteoblasts showed a typical flat shape on this surface as well, and they completely covered the sharp tops of the small pyramids (Fig. 7B). The rough pyramid shaped surface formed after prolonged etching in KOH solution as well as sandblasted surfaces led to a different morphology of the attached MG-63 cells. The cells followed the structures of the etched surface but appeared smaller than those on smooth surfaces. The cells covered partly or entirely several cavities, and mostly revealed contacts at the edges or tops of the pyramids. Continuous contact of the entire cell surface to the rough wafer surface occurred only very rarely, if at all (Fig. 7C). Likewise, MG-63 cells tolerated the rock-like surface structure of sandblasted wafers. However, the relatively small cells spanned across the sharp ridges, and cell contact to the surface appeared discontinuous (Fig. 7D).

Discussion

Proliferation of adhesion-dependent cells is influenced by surface properties such as chemistry, free energy, charge, wettability, and topography of material surfaces. Here, we used MG-63 osteoblasts representative for cells derived from bone tissue and 3T3 fibroblasts from connective tissue to study the proliferation and morphology of cells on SAMs of organosilanes and on rough surfaces. The cells of both cell lines proliferated on all wafer surfaces. However, the number of cells observed was depended on the chemistry of the surfaces. High proliferation of osteoblasts occurred on oxidized surfaces (Ox), NH_2-terminated surfaces (APS), and hydrophobic CH_3-terminated surfaces (OTS), while PEG-modified surfaces induced slightly lower cell numbers after an incubation period of 8 days. Cell proliferation was very slow on hydrophobic CF_3-terminated

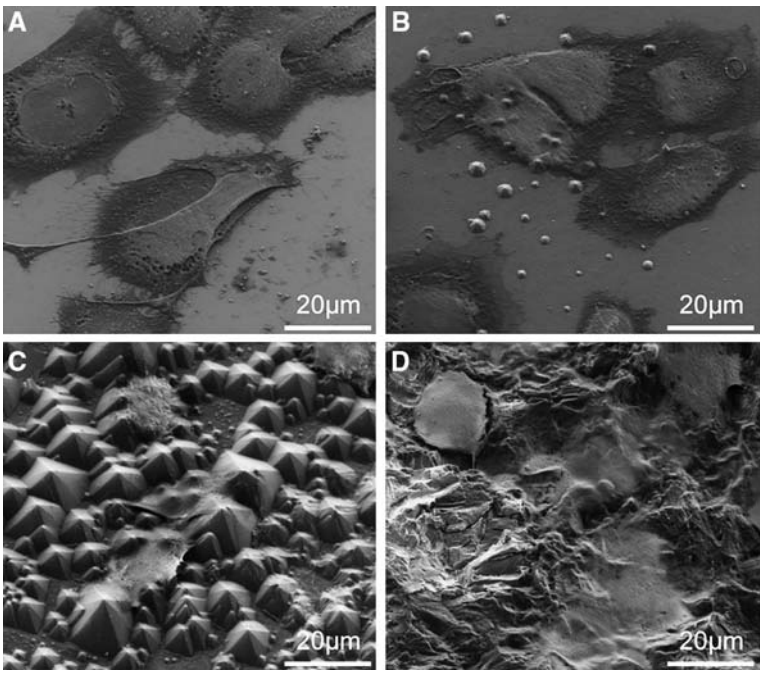

Fig. 7 Scanning electron micrographs of human MG-63 osteoblasts on smooth and rough silicon wafers. The cell morphology was analyzed on an oxidized smooth wafer surface (**A**), a surface etched in 10% aqueous potassium hydroxide solution for 5 min (**B**), a surface etched in 10% aqueous potassium hydroxide solution for 60 min (**C**), and a surface sandblasted with corundum particles (**D**). The cells appear extremely flattened on a smooth wafer surface (**A**) and on a surface etched in KOH for 5 min (**B**). The morphology of the cells changed on surfaces etched in KOH for 60 min (**C**), and a sandblasted surface (**D**). There is no continuous contact between the cells and the wafer surface for KOH 60 and SB, and the cells span across the ridges

surfaces (HFS). SEM images clearly supported this observation since very few osteoblasts appeared on HFS immediately after seeding and the cells were extremely rounded with almost no indication of cell attachment to the surface. The proliferation of 3T3 fibroblasts on SAMs was very similar to that detected for osteoblasts. The number of fibroblasts on APS was significantly higher compared with all other surfaces, but lower on HFS.

Our results are in agreement with previously published observations. It has been repeatedly reported that cell adhesion and proliferation depends on surface chemistry, and varies with individual functional groups rather than general surface properties like wettability [3–7, 9, 21]. For instance, cell behavior was analyzed on SAMs of alkyl silanes that were terminated with hydrophobic groups like methyl (CH_3) and vinyl ($CH_2 = CH_2$) groups. The introduction of amine (NH_2) and carboxyl (COOH) groups created moderately wettable surfaces, and the application of poly(ethylene glycol) (PEG) and hydroxyl (OH) groups lead to hydrophilic surfaces. It seemed that adhesion of human fibroblasts on the hydrophobic CH_3 as well as on hydrophilic PEG and OH terminated SAMs was weak. In contrast, strong attachment, spreading, and cell proliferation as well as enhanced formation of a fibronectin matrix, was detected on moderately hydrophobic COOH and NH_2 groups [7]. Likewise, myoblast proliferation and differentiation was characterized on alkanethiol SAMs terminated with OH, CH_3, NH_2, and COOH groups. It appeared that the hydrophilic OH surface as well as the CH_3 group supported selective binding of $alpha_5beta_1$ integrin, while the moderately hydrophobic COOH and NH_2 groups bound to both $alpha_5beta_1$ and $alpha_Vbeta_3$ again indicating the relevance of functional groups for cell proliferation [9]. High cell proliferation was detected on a relatively hydrophobic NH_2-modified surface compared with cell behavior on OH- or COOH-terminated SAMs [22]. On the other hand, cell adhesion and proliferation was also high on charged COOH with respect to a more hydrophobic CH_3-terminated surface [9, 23–25]

Our findings show that the uncoated hydrophobic fluorocarbon surfaces (HFS) strongly inhibited cell adhesion and proliferation compared with a hydrophobic CH_3–terminated surface (OTS) surface. The degree of cell proliferation on both hydrophobic surfaces is influenced by the different functional groups. An otherwise unchanged hydrocarbon surface (OTS) may be more suitable for initial cell contact because of hydrophobic interactions between the hydrocarbon coating and hydrocarbon moieties of fatty acids or proteins of the cell membrane. In contrast, cell proliferation on HFS may be delayed because of a poor interaction of the hydrocarbon moieties on the cell surface and fluorocarbon wafer surfaces. The relative high cell number, even on HFS after a longer incubation period, may be a consequence of the production of the cells own extracellular matrix which then is a suitable substrate to facilitate proliferation. Similar to our observations, human skin fibroblast adhesion was reduced on hydrophobic CF_3-modified glass surfaces, which was considered to have low tissue compatibility because of the high number of rounded and non-proliferating cells that were detected [22]. However, even this non-adhesive surface allowed limited cell adhesion over time, although the differences compared to other surfaces were much smaller than those seen in our study [22, 26]. Thus, it appears that HFS-terminated surfaces have potential for clinical applications

when blood-contacting materials like cardiovascular devices, vascular grafts and stents are required. However, a more comprehensive evaluation of its usefulness, as a coating for medical devices, will require future studies using clinically relevant materials like polymers or composite materials. In addition, the adhesion of other relevant eukaryotic cells including cells of the immune system as well as pathogenic microbial organisms needs to be determined.

Cell adhesion on biomaterial surfaces in vivo is mediated through proteins from complex fluids like serum, blood or saliva. The biochemical kinetics of the adsorption of proteins from serum or saliva on biomaterials is faster than the attachment of cells or bacterial cells. Thus, the surface characteristics of biomaterials available for cell adhesion and cell proliferation are modified or often masked by the properties of an adsorbed protein layer [1, 27]. It is well documented that serum contains proteins like fibronectin and vitronectin which support cell adhesion to surfaces. Unlike proteins such as fibronectin and vitronectin, other serum proteins like albumin lack cell specific domains, and thus do not support the receptor-mediated binding of cells to biomaterials [1, 27, 28].

In our study, precoating of the wafer surfaces with cell culture serum inhibited the proliferation of MG-63 osteoblasts on all surfaces except HFS, especially after a long incubation period of 8 days. Yet, cell proliferation on serum-coated HFS was still lower than on other SAMs, and the proliferation of 3T3 fibroblasts appeared to be slightly inhibited on HFS. Adhesive proteins like fibronectin or vitronectin may have an effect particularly on cell adhesion on HFS surfaces, but they were not studied here. It has been reported, that vitronectin was a key component of proteins adsorbed from bovine serum to SAMs. It also appeared as if less protein adsorbed to PEG and OH compared with CH_3, NH_2 and COOH surfaces. Adsorption of fibronectin to SAMs, however, was not detected by SDS-PAGE [7]. The identification of the masses and the particular species of proteins on these surfaces is currently under investigation using modern protein chemical microscale methods. The influence of serum proteins on cell adhesion and proliferation has been investigated previously with varying results [7, 21, 24, 25, 29, 30]. Attachment of 3T3 fibroblasts was significantly higher on hydrophilic model silane surfaces with diluted serum preadsorbed [21, 31]. In contrast, osteoblast attachment in serum-free medium was significantly reduced on COOH, OH, and CH_3 surfaces after preadsorption of albumin, a major component of serum [25]. Discrepancies in the adhesion and proliferation of cells between otherwise identical SAMs may also be related to the use of different cell lines. For instance, the presence of serum proteins influenced the proliferation of epithelial cells on SAMs, and cell growth was not inhibited on hydrophobic surfaces exhibiting CH_3 and CF_3 functional groups [29].

Surface topography or texture is another property which influences the functional activity of cells in direct contact with an implant material. Model surfaces are again ideal tools for studying the effects of this surface topography without changing the chemical characteristics of the surfaces [14]. Here, chemical etching in caustic solution produced a unique texture on the wafer surface which, to our knowledge, has not yet been used as a substrate for the analysis of cell adhesion or proliferation thus far. The KOH solution created a pyramid-shaped wafer surface, with the size of the pyramids increasing as a function of etching time. Notable is that the average roughness of wafer surfaces etched in KOH solution for 60 min was the same as that produced by sandblasting with corundum particles. However, the texture of each surface was completely different. Recent findings indicated that surface morphology was even more important for long-term adhesion and the proliferation capacity of cells than material composition or surface roughness [16, 17, 32, 33].

Our scanning electron micrographs showed that MG-63 osteoblasts clearly distinguished between the roughness and the different textures of the wafer surfaces. The osteoblasts spread well on smooth surfaces and those with a few small pyramids created after etching in caustic solution for a short period of time. Moreover, the many filopods indicated a close and solid contact to these surfaces. In contrast, osteoblasts appeared smaller on the very rough pyramid-shaped surface as well as on the rough sandblasted surface with sharp ridges and edges, although these rough surfaces with different textures were also tolerated. However, there was no continuous contact between the cells and the wafer surfaces, and the cells spanned across narrow cavities as if they failed to recognize the steep and rough terrain. Similarly, it has been previously reported that cells spread on the ridge of narrow grooves (smaller than 2 μm) with only few focal contacts, whereas on the wider grooves (wider than 5 μm), the substrate surface was completely covered by cells [34]. MG-63 osteoblasts distinguish between surfaces with 10, 30, and 100 μm wide hemispherical cavities. The cells span cavities with small diameters but are able to grow down into cavities as wide as 30 and 100 μm to cover the bottom of the cavities [14, 18]. Based on these findings, it appears that the quality of cell contact on rough surfaces is related to the minimum width of the cavity. It is possible that osteoblasts with a size of about 20–30 μm needed at least the same width of a cavity between the peaks or edges of the rough pyramid-shaped surfaces to make continuous contact to the surface. This observation has been described before by other authors [14, 15, 18, 34].

Here, the silicon wafer surfaces with different roughness and topography did not influence the number of MG-63 osteoblasts and 3T3 fibroblasts after an incubation period of

up to 8 days. Nor was any effect detected from precoating the silicon surfaces with serum. Our results are in agreement with other observations that MG-63 cell proliferation was not affected by nanoscale and microscale surface roughness of titanium disks. Nevertheless, a synergistic effect was described when combining nano- and micro-structured surfaces [14, 18]. On the other hand, it has been reported that the topography of a surface may influence cell proliferation and cell differentiation. It appears that cell proliferation was inhibited on micro-rough surfaces, which in turn favored cell differentiation [10, 12, 35, 36]. It is assumed in the field of dental research that the use of implant materials with rough surfaces may lead to predictable bone integration. However, the results thus far have only been obtained from short-term investigations based on autoradiography and clinical observations [37]. It has been reported that nano-structured surfaces selectively enhanced adhesion of osteoblasts on surfaces compared with fibroblasts [38]. Cell adhesion, however, may also vary depending on the type of cell. For instance, studies have shown that more human gingival fibroblasts or periodontal cells may attach to smooth surfaces than to rough surfaces [39, 40].

Conclusion

Based on the results of the present investigation, we conclude that differences in cell proliferation on SAMs of alkylsilanes depend more on the chemistry of the terminating groups than on wettability. Cell proliferation on hydrophobic surfaces like OTS is as high as that on moderately hydrophobic surfaces (APS) and hydrophilic oxidized surfaces. It is also evident that cell proliferation on hydrophobic surfaces like hydrocarbon (OTS) and fluorocarbon (HFS) is completely different. Cell morphology on fluorocarbon surfaces (HFS) indicates very weak initial cell-surface contact, although surfaces of different roughnesses and textures are recognized by MG-63 osteoblasts. The cells spread well on smooth surfaces but appear smaller on rough and unique pyramid-shaped surface and on rough sandblasted surfaces with sharp ridges and edges. It appears that the quality of cell contact on rough surfaces is related to the minimum width of the cavity.

Acknowledgments We would like to thank B. Bey, H. Ebensberger, U. Renner, W.Q. Zhou, J. Vancea, R. Held, and M. Kreuzer for their excellent technical assistance, and the Medical Faculty of the University of Regensburg for financial support.

References

1. K. ANSELME, *Biomaterials* **21** (2000) 667
2. K. ANSELME and M. BIGERELLE, *Biomaterials* **27** (2006) 1187
3. Y. TAMADA and Y. IKADA, *J. Biomed. Mater. Res.* **28** (1994) 783
4. G. ALTANKOV, F. GRINNELL and T. GROTH, *J. Biomed. Mater. Res.* **30** (1996) 385
5. H. DU, P. CHANDAROY and S. W. HUI, *Biochim. Biophys. Acta.* **1326** (1997) 236
6. T. GROTH, B. SEIFERT, G. MALSCH, W. ALBRECHT, D. PAUL, A. KOSTADINOVA, N. KRASTEVA and G. ALTANKOV, *J. Biomed. Mater. Res.* **61** (2002) 290
7. N. FAUCHEUX, R. SCHWEISS, K. LUTZOW, C. WERNER and T. GROTH, *Biomaterials* **25** (2004) 2721
8. B. G. KESELOWSKY, D. M. COLLARD and A. J. GARCIA, *Biomaterials* **25** (2004) 5947
9. M. A. LAN, C. A. GERSBACH, K. E. MICHAEL, B. G. KESELOWSKY and A. J. GARCIA, *Biomaterials* **26** (2005) 4523
10. C. H. LOHMANN, E. M. TANDY, V. L. SYLVIA, A. K. HELLVOCKE, D. L. COCHRAN, D. D. DEAN, B. D. BOYAN and Z. SCHWARTZ, *J. Biomed. Mater. Res.* **62** (2002) 204
11. B. D. BOYAN, S. LOSSDORFER, L. WANG, G. ZHAO, C. H. LOHMANN, D. L. COCHRAN and Z. SCHWARTZ, *Eur. Cell. Mater.* **6** (2003) 22
12. M. MANTE, B. DANIELS, E. GOLDEN, D. DIEFENDERFER, G. REILLY and P.S. LEBOY, *J. Oral. Implantol.* **29** (2003) 66
13. S. LOSSDORFER, Z. SCHWARTZ, L. WANG, C. H. LOHMANN, J. D. TURNER, M. WIELAND, D. L. COCHRAN and B. D. BOYAN, *J. Biomed. Mater. Res.* **70A** (2004) 361
14. O. ZINGER, K. ANSELME, A. DENZER, P. HABERSETZER, M. WIELAND, J. JEANFILS, P. HARDOUIN and D. LANDOLT, *Biomaterials* **25** (2004) 2695
15. F. LUTHEN, R. LANGE, P. BECKER, J. RYCHLY, U. BECK and J. G. NEBE, *Biomaterials* **26** (2005) 2423
16. D. BUSER, T. NYDEGGER, T. OXLAND, D. L. COCHRAN, R. K. SCHENK, H. P. HIRT, D. SNETIVY and L. P. NOLTE, *J. Biomed. Mater. Res.* **45**(2) (1999) 75
17. K. ANSELME, M. BIGERELLE, B. NOEL, E. DUFRESNE, D. JUDAS, A. IOST and P. HARDOUIN, *J. Biomed. Mater. Res.* **49** (2000) 155
18. O. ZINGER, G. ZHAO, Z. SCHWARTZ, J. SIMPSON, M. WIELAND, D. LANDOLT and B. BOYAN, *Biomaterials* **26** (2005) 1837
19. L. D. DYER, G. J. GRANT, C. M. TIPTON and A. E. STEPHENS, *J. Electrochem. Soc.* **136** (1989) 3016
20. R. J. GILLES, N. DIDIER and M. DENTON, *Anal. Biochem.* **159** (1986) 109
21. K. WEBB, V. HLADY and P. A. TRESCO, *J. Biomed. Mater. Res.* **49** (2000) 362
22. G. ALTANKOV, K. RICHAU and T. GROTH, *Mat.-wiss. U. Werkstofftech.* **34** (2003) 1120
23. C. D. TIDWELL, S. I. ERTEL and B. D. RATNER, *Langmuir* **13** (1997) 3404
24. K. B. MCCLARY, T. UGAROVA and D. W. GRAINGER, *J. Biomed. Mater. Res.* **50** (2000) 428
25. C. A. SCOTCHFORD, C. P. GILMORE, E. COOPER, G. J. LEGGETT and S. DOWNES, *J. Biomed. Mater. Res.* **59** (2002) 84
26. T. O. ACARTURK, M. M. PEEL, P. PETROSKO, W. LAFRAMBOISE, P. C. JOHNSON and P. A. DIMILLA, *J. Biomed. Mater. Res.* **44** (1999) 355
27. C. J. WILSON, R. E. CLEGG, D. I. LEAVESLEY and M. J. PEARCY, *Tissue. Eng.* **11** (2005) 1
28. A. S. G. CURTIS and J. V. FORRESTER, *J. Cell. Sci.* **71** (1984) 17
29. M. FRANCO, P. F. NEALEY, S. CAMPBELL, A. I. TEIXEIRA and C. J. MURPHY, *J. Biomed. Mater. Res.* **52** (2000) 261

30. P. FILIPPINI, G. RAINALDI, A. FERRANTE, B. MECHERI, G. GABRIELLI, M. BOMBACE, P. L. INDOVINA and M. T. SANTINI, *J. Biomed. Mater. Res.* **55** (2001) 338
31. K. WEBB, V. HLADY and P. A. TRESCO, *J. Biomed. Mater. Res.* **41** (1998) 422
32. F. COOPER, *J. Prosthetic. Dentist.* **84** (2000) 522
33. M. BIGERELLE and K. ANSELME, *J. Biomed. Mater. Res. A* **72A** (2005) 36
34. K. MATSUZAKA, X. F. WALBOOMERS, M. YOSHINARI, T. INOUE and J. A. JANSEN, *Biomaterials* **24** (2003) 2711
35. J. Y. MARTIN, Z. SCHWARTZ, T. W. HUMMERT, D. M. SCHRAUB, J. SIMPSON, J. LANKFORD, D. D. DEAN, D. L. COCHRAN and B. D. BOYAN, *J. Biomed. Mater. Res.* **29** (1995) 389
36. K. KIESWETTER, Z. SCHWARTZ, T. W. HUMMERT, D. L. COCHRAN, J. SIMPSON, D. D. DEAN and B. D. BOYAN, *J. Biomed. Mater. Res.* **32** (1996) 55
37. Z. SCHWARTZ, E. NASAZKY and B. D. BOYAN, *Alpha. Omegan.* **98** (2005) 9
38. R. L. PRICE, K. ELLISON, K. M. HABERSTROH and T. J. WEBSTER, *J. Biomed. Mater. Res.* **70A** (2004) 129
39. M. KÖNÖNEN, M. HORMIA, J. KIVILAHTI, J. HAUTANIEMI and I. THESLEFF, *J. Biomed. Mat. Res.* **26** (1992) 1325
40. D. COCHRAN, J. SIMPSON, H. WEBER and D. BUSER, *Int. J. Oral. Maxillofac. Implants.* **9** (1994) 289